Challenges and perspectives of functional sodium imaging (fNaI)

Claudia AM Gandini Wheeler-Kingshott*[1,2,3], Frank Riemer*[1,4], Fulvia Palesi[5], Antonio Ricciardi[1], Gloria Castellazzi[1,6] Xavier Golay[7], Ferran Prados[8], Bhavana Solanky[1], Egidio U D'Angelo[2,9]

*Equally contributed to this work

[1]NMR Research Unit, Queen Square MS Centre, Department of Neuroinflammation, UCL Institute of Neurology, Factulty of Brain Sciences, University College London, London, UK
[2]Department of Brain and Behavioural Sciences, University of Pavia, Pavia, Italy
[3]Brain MRI 3T Mondino Research Center, IRCCS Mondino Foundation, Pavia, Italy
[4]Department of Radiology, School of Clinical Medicine, University of Cambridge, Cambridge, United Kingdom
[5]Neuroradiology Unit, IRCCS Mondino Foundation, Pavia, Italy
[6]Department of Electrical, Computer and Biomedical Engineering, University of Pavia, Pavia, Italy
[7]NMR Research Unit, Queen Square MS Centre, Department of Brain Repair and Rehabilitation, UCL Institute of Neurology, Factulty of Brain Sciences, University College London, London, UK
[8] FERRAN
[9]Brain Connectivity Centre, IRCCS Mondino Foundation, Pavia, Italy

Abstract
Brain function has been investigated via the blood oxygenation level dependent (BOLD) effect using magnetic resonance imaging (MRI) for the past decades. Advances in sodium imaging offer the unique chance to access signal changes directly linked to sodium ion (23Na) flux across the cell membrane, which generates action potentials, hence signal transmission in the brain. During this process, sodium ions (23Na) transiently accumulate in the intracellular space. Here we show that functional sodium imaging (fNaI) at 3T is sensitive to sodium ion (23Na) concentration changes during finger tapping, which can be quantified in grey and white matter regions key to motor function. For the first time, we measured a sodium ion (23Na) concentration change of 0.54 mmol/l in the ipsilateral cerebellum, 0.46 mmol/l in the contralateral primary motor cortex, 0.27 mmol/l in the corpus callosum and -11 mmol/l in the ipsilateral primary motor cortex, suggesting that fNaI is sensitive to both excitation and inhibition and to sodium concentration changes in white matter, where BOLD fails. Initial calculations from neuronal ATP consumption can explain 10% of the experimental change, with the remainder potentially reflecting blood volume changes. An open issue persists in the role of the glymphatic system in maintaining homeostasis and volume distributions during neuronal activity. Development of realistic models of tissue function will be essential to understand the mechanisms of such changes

and contribute to meeting the overarching challenge of measuring neuronal activity *in vivo*.

Introduction

Ever since the blood oxygenation level dependent (BOLD) effect was described, functional magnetic resonance imaging (fMRI) has dominated neuroscience as the method for indirectly measuring brain activity (Ogawa et al., 1990b, 1990a, 1992). It allows mapping of magnetic resonance (MR) signal changes generated by the mismatch between oxygen delivery and consumption upon neuronal activation. While this approach has provided significant insight into brain function, a major limitation of the BOLD technique is that it does not directly measure neuronal activity and is affected by subject specific haemodynamic factors. Thus, an approach that could directly measure whole brain neuronal activity in humans *in vivo*, non-invasively, and that would depend less on background cerebrovascular factors unrelated to neuronal function, would have a major advantage over BOLD-fMRI and would possibly contribute to improved functional localisation.

In this paper, we propose that, due to sodium MRI technology, we are within reach of measuring directly a key component of neuronal activity, which is a local transient change of sodium ions (23Na) concentration in the intracellular space. During activity there is, indeed, an increased sodium ions (23Na) flux between the extracellular and intracellular space characterised by a temporal scale of several milliseconds, which causes the shift in sodium ion (23Na) concentrations. If sodium imaging, dynamically repeated, was successful in detecting sodium ions (23Na) concentration changes evoked by specific tasks, it would open up a new and much more direct way of investigating human brain function in health and disease conditions, complementing BOLD fMRI.

BOLD signal is also insensitive to functional changes in white matter primarily due to its low cerebral blood volume. As a matter of fact, imaging of other aspects of the brain electrical activity, such as those related to transmembrane sodium-potassium ion exchange during depolarization, would provide a more direct access to primary brain function. Although sodium channels are predominantly located in the axonal initial segment (Chadderton et al., 2004; Dover et al., 2016; Häusser and Clark, 1997; Masoli et al., 2015; Powell et al., 2015; Rancz et al., 2007) where action potentials are activated, nodes of Ranvier are also present along white matter fibres. Indeed, white matter BOLD signal is hard to detect as the vascularization of white matter is negligible compared to grey matter, hence the contribution of the nodes of Ranvier to signal conduction along the axons is not accessible with BOLD fMRI. This is particularly problematic as it has been proposed that the largest energy demand related to brain function is related to the post-depolarization sodium-potassium pump to re-establish neuronal membrane potential (Brockhaus et al., 1993; Koch and Barish, 1994). Measuring sodium ion (23Na) concentration changes could potentially be sensitive to alterations in white matter tracts implicated in supporting targeted functions and contribute to our understanding of the brain circuits involved in specific tasks.

Despite its limitations, BOLD fMRI has been very successful in neurological research applications, for example to study mechanisms of disease. Pathologies where blood perfusion is impaired, such as multiple sclerosis (Paling et al., 2013) and stroke (Sakatani et al., 2007), reveal alterations in functional response to stimuli during BOLD fMRI. However, this can be difficult to interpret since these alterations may be mediated by a dysfunction in evoked blood oxygenation or by neuronal damage itself. Experimental neurophysiology also indicates that psychiatric conditions, such as autism, are characterised by altered patterns of neuronal firing, which are posing mechanistic questions difficult to fully interpret from changes in an indirect measure such as BOLD fMRI (Giza et al., 2010; Leblond et al., 2014). Considering its substantial research output, BOLD fMRI is rarely used clinically, outside of pre-surgical planning of tumour resections, epilepsy and functional surgery. Yet, while there is a growing evidence that minimising residual tumour mass improves survival, false functional localisation may render it less effective than one wished it to be, albeit while having shown that it improves post-intervention outcomes (Morrison et al., 2016; Suchorska et al., 2016). This means that there is a clear and pressing need to develop tools able to more directly map brain function, rather than secondary haemodynamic effects, and with greater reliability, to improve clinical practice. Again, measuring sodium ions (23Na) concentration changes during function could complement BOLD fMRI providing a more direct measure of brain function, with the potential of impacting clinical practice.

Recent physiological discoveries suggest that it may be possible to develop alternative strategies to measure brain function in vivo "if" it was possible to measure evoked changes in sodium ion (23Na) concentrations during brain function. The functioning of neuronal cells has recently been mapped *in vitro* with high specificity, describing distribution and functionality of sodium channels in neurons with incredible details (Dover et al., 2016; Masoli et al., 2015). In parallel, physiological studies have also led to a better understanding of neurovascular coupling (Howarth et al., 2009; Mapelli et al., 2016), which is assumed to be at the origin of the BOLD fMRI signal (Ogawa et al., 1990b, 1990a, 1992). These data are the bases for constructing emerging realistic models of neuronal activity, built on ever accurate physiological recordings of cellular function, and provide an invaluable tool to assess and interpret large scale measures of brain function from MRI (D'Angelo and Wheeler-Kingshott, 2017).

In parallel to physiological discoveries, technology advances have made it feasible to measure sodium ion (23Na) concentrations *in vivo*, which are key in retaining physiologically balanced tissues. Indeed, it is now possible, at least in the research environment, to non-invasively measure quantitatively total (i.e. intra + extra cellular) sodium ion (23na) concentrations (TSC) of the human brain tissue *in vivo* using high field (3T and above) MRI scanners (Thulborn, 2018). Sodium ions (23Na) have a spin 3/2, which means that sodium ions are MR visible. Given their different gyromagnetic ratio and spin, their Larmor frequency is lower than that of the proton (1H), which is the source of common MRI images. Therefore, with appropriate coils, tuned to the Larmor frequency of the sodium ions (23Na), it is possible to measure TSC *in vivo* in humans (Thulborn, 2018). Furthermore, sodium ions (23Na) in the intra and extracellular spaces have different MR

properties due to their cellular environment, hence any alteration in volume fractions or in intra or extracellular sodium ions (23Na) concentrations could affect the measured TSC. Arguably one could say that TSC is sensitive to changes due to tissue composition (e.g. in grey matter or white matter) as well as to pathological changes of tissue cellularity, albeit with a lower sensitivity than proton (1H), or indeed due to transient changes of sodium ions (23Na) concentration during functional activity.

With preliminary data and biophysical hypothesis of sodium ions (23Na) concentration changes (ΔTSC) in tissue *in vivo*, we intend to establish a framework for developing functional sodium imaging (fNaI), demonstrating an exciting opportunity for measuring neuronal activity, and addressing a pressing need for a multi-disciplinary integration.

Methods

Subjects: 8 right-handed healthy volunteers (mean age 33yrs, range 27-45, 5 males) gave written consent to this study approved by our local ethics committee.

fNaI acquisition protocol: Data was acquired on a 3T Philips Achieva system (Philips, Netherlands) with a single-tuned volume head-coil (Rapid, Germany) using a 4-times undersampled 3D-Cones ultra-short echo time sequence (Gurney et al., 2006; Riemer et al., 2014), 4 mm isotropic resolution, 240 mm field-of-view, 90° flip-angle, TR = 50ms, TE = 0.22 ms, 6 NEX, total scan time per volume = 60s.

fNaI paradigm design: fNaI was performed back-to-back 6-times during which the subject was asked (verbally) to alternately rest or perform a right-hand finger-tapping task (self-pacing at a frequency = 1Hz). Subjects performed the task by tapping the thumb to each one of the fingers, repeatedly from the index to the little finger and back to the index, with ample extension of the movements, for a continuous 60s. Instructions of tapping or resting were given verbally by the operator through the intercom of the scanner.

fNaI data analysis: Images were reconstructed to 2mm isotropic resolution using SNR-enhancing sub-Nyquist k-space sample weighting (Pipe, 2000). All analyses were performed with SPM8. Images were rigidly registered, smoothed with a 8x8x8mm^3 Gaussian-kernel and normalised to the proton density (PD) MNI152 template. Statistical analysis was performed using the PET group analysis toolbox. Statistical maps were calculated with p=0.001, cluster extent of k = 20 voxels and family-wise error (FWE) correction.

fNaI clusters identification: Maps of t-statistics were saved from the fNaI data analysis and imported in the xjview toolbox (http://www.alivelearn.net/xjview) of SPM to obtain a full detailed report for each resulting cluster in terms of peak, number of voxels, location and anatomical areas involved in Tailarach atlas space (Yoon et al., 2012).

Sodium ions (23Na) flux and ΔTSC: Sodium quantification was performed according to Christensen JD et al. (Christensen et al., 1996), using two reference

phantoms (33 and 66 mmol/l sodium agar) placed either side of the brain for 4 out of 8 volunteers. Clusters of activation were unwarped and applied as masks to the TSC average on/off maps obtained in native space for each subject. Mean and standard deviation were calculated for the cerebellar, ipsi and contralateral primary motor cortex and corpus callosum clusters and reported in terms of their mean ΔTSC.

Results

fNaI was successfully performed in 8 subjects during a right-hand finger-tapping task (frequency = 1Hz), at 3T using an acquisition sequence sensitive to total sodium concentration changes, i.e. to ΔTSC. Figure 1a) shows transverse slices from one fNaI volume of a randomly chosen subject, while Figure 1b) shows fNaI statistical activation maps from the group analysis. A total of 16 main clusters were identified. Table 1 reports the MNI coordinates for the activation peak of each cluster in Talairach space, the location of the peak and a list of sub-areas contained in each cluster. These include the contralateral primary motor (Precentral), somatosensory (Postcentral) and supplementary motor (Superior Frontal) gyri, and the ipsilateral anterior cerebellum (lobule I-IV) as well as lobule VI, Crus I-II and the dentate nucleus (Figure 1c)). Noticeable are the large number of ipsilateral areas that were also activated in the ipsilateral cerebrum (e.g., frontal and temporal lobes, postcentral gyrus, deep grey matter including the right thalamus, the insular cortex, the limbic lobe and parahippocampal gyrus. The lingual gyrus, Broadmann areas (BA) 2, 19 and 37 were also activated ipsilaterally to the movement). Interestingly, white matter areas were identified in the corpus callosum, as well as in the contralateral paracentral lobule and the medial frontal gyrus, the corticospianl tract, the posterior cingulum and in the ipsilateral supramarginal gyrus.

ΔTSC in the anterior cerebellar cluster from fNaI was measured to be (0.54 ± 0.17) mmol/l, while it was (0.27 ± 0.08) mmol/l in the corpus callosum, (0.46 ± 0.10 mmol/l in the contralateral primary motor cortex, while a negative ΔTSC change was measured in the ipsilateral primary motor cortex (-0.11 ± 0.06) mmol/l.

Discussion

Here, we have shown preliminary evidence that brain function can be assessed non-invasively by sodium imaging *in vivo* using a 3T MRI scanner, a major step forward in the overarching aim to directly assess neuronal activity. Indeed, fNaI successfully detected changes in activation between two states, i.e. finger tapping and rest, across the entire brain. Activations in motor areas as well as in areas known to contribute to executive functions and motor control indicate that fNaI has the potential to be an effective biomarker of functional activity. Measured quantitative ΔTSC are consistent between regions and offer a robust starting point to investigate physiological processes at the basis of quantitative fNaI. Although the present data is only a proof of principle, results are exciting and could open a new era in functional imaging of the human brain.

The localisation of the activated regions is conveying very interesting results worth discussing, in light of future study design and development. Several clusters are at the border between grey and white matter, where one would indeed expect the greatest accumulation of intracellular sodium, due to the high concentration of sodium channels in the axon initial segment where it connects to the soma (Dover et al., 2016). The task employed in this initial experiment was indeed demanding: one minute of finger tapping requires motor planning and concentration, especially as subjects were asked to self-pace at 1Hz. Interestingly, as well as the primary motor cortex (BA4), the study shows activations in the primary somatosensory cortex (BA2), i.e. the main cortical area for processing the sense of touch, and in the premotor cortex (BA6), which is involved (with the cerebellum) in self-pacing finger tapping (Mak et al., 2016; Witt et al., 2008). In the cerebellum, activations occurred in posterior ipsilateral areas, namely Crus I/II, lobule VI, and lobule VIIIa, which are heavily involved in integrative aspects of motor control and cognitive processing (Mak et al., 2016; Witt et al., 2008). A striking finding, though, is that we have detected patches of activity in white matter regions, including: the corticospinal tract, the superior longitudinal fasciculus, the corpus callosum, the mid portion of the cingulum and the superior and inferior cerebellar peduncles. The corticospinal tract is the major pathway for the motor system; the superior longitudinal fasciculus connects parietal to prefrontal cortices and is known to be part of associative fibres that integrate information of body awareness and perception; the corpus callosum is the main pathway to connect both hemispheres while the cingulum receives afferent fibres from the thalamus, as part of the spino-thalamic tract; the superior cerebellar peduncle is the gateway of the cerebro-cerebellar loop for the efferent fibres from the cerebellum to the cortex, while the inferior cerebellar peduncle is the gateway for fibres connecting the spinal cord and the cerebellum, forming a key pathway for integrating proprioceptive sensory inputs. These tracts are myelinated and enriched in sodium channels at the nodes of Ranvier, and do not show BOLD signal in response to fMRI tasks, but are indeed forming the axonal pathways wiring-up the sensorimotor network involved in finger tapping. Reconstruction of axonal circuits supporting functions would therefore find invaluable information in white matter fNaI results.

From the present data it is impossible, though, to determine the mechanisms underlying fNaI changes, i.e. to assess whether ΔTSC reflects sensitivity mainly to the shift of sodium ions between the intracellular and extracellular compartments, $\Delta[23Na]_i/\Delta[23Na]_e$ (Gilles et al., 2017). A main question is whether fNaI changes are also reflecting the change in the vascular and perivascular spaces, especially in grey matter, associated with an increased blood volume due to neurovascular coupling between glucose metabolism and increase blood delivery; in other words, we cannot exclude that in the present measurements, a significant contribution comes from the blood compartment. Although this criticism is one of the most obvious to put forward, there are strong reasons to believe that changes in blood flow and volume are not the only contributors of this exploratory study.

Whilst a precise estimate would require sophisticated models and combinations of experimental measurements *in vivo* and *in vitro*, here we can probe likely/expected scenarios and propose some *ab initio* calculations. The first issue

is to determine whether the molar flux of sodium ions displaced during activity is sufficient to generate a meaningful fNaI signal. On one hand, the approximate calculation based on known electrophysiology measurements of ATP consumption in the cerebellar cortex supports that ionic transfer of sodium explains at least 10% of the measured signal. In the cerebellum, our feasibility study measured a ΔTSC of 0.54 ± 0.17 mmol/l between active and rest states. The ATP consumption of neurons in the cerebellar cortex has been measured to be 20.5 mmol of ATP / g · min (Howarth et al., 2009, 2012; Sokoloff et al., 1977). Of this ATP, 50% is used for computation while the other 50% for maintenance (Brockhaus et al., 1993; Koch and Barish, 1994; Howarth et al., 2009, 2012), so about 10 mmol of ATP / g * min are used for function. 1 ATP corresponds to shifting three sodium ions (previously accumulated inside the cell) through the cell membrane to re-establish ionic balance; this means that during activity there is a shift of the order of 30E-3 mmol of 23Na / g · min, i.e. 0.03 mmol of sodium / l · min, which is 10 times smaller than our measured value. What other sources of sodium flux should we consider to explain our experimental in vivo fNaI data? A recent study, proposed in abstract form, suggests that fNaI signal comes mainly from a generic "reduction" of extracellular sodium, although no quantitative measures are provided (Ranjeva et al., 2018). It is important, also, to assess the contribution of changes in cerebral blood volume (CBV) during brain function and changes in Virchow-Robin spaces volume (VRSV) through the glymphatic system. It has been shown that the major contribution to CBV changes during functional activation comes from the arteriole (CBVa), where CBVa at rest is of the order of 0.8 mmol/100g, with a change of CBVa due to activity of ΔCBVa = 0.34 mmol/100g(Hua et al., 2011; Kim et al., 2007; Lee et al., 2001). This is translated to the capillary bed, where the venous side passively follows the arterioles dilation and resistance changes that induce blood flow and volume changes (Buxton, 2012) If ΔCBVa is added to the extracellular space compartment, reducing the cellular volume fraction even by as little as 0.5%, this would be enough to cause a molar change in TSC of the order of the measured one, i.e. 0.43 mmol/L, because of the 10 times higher molar concentration of sodium ions (23Na) outside compared to inside neuronal cells. This ΔCBVa, though, would not affect the ΔTSC measured if its fractional volume was balanced by a corresponding reduction in VRSV, i.e. if the extracellular space (CBV + extracellular matrix + VRSV) and the cellular space (e.g. intracellular space + myelin) proportions remained constant (e.g. 20% and 80% respectively). In this hypothesis, the perivascular space and therefore the glymphatic system, would work as a compensatory chamber and the neuronal structures would be "rigid" within the extracellular matrix (Thulborn, 2018). The role of cerebrovascular fluid (CSF) in buffering the changes in CBV during functional activity has been investigated and reported to be reduced during activation, using relaxometry in the visual cortex, and could support this hypothesis (Piechnik et al., 2009).

On the other hand, we must not forget that the ΔTSC measured experimentally in this study *in vivo* is an "apparent" TSC change, as the current acquisition protocol cannot distinguish between the intra and extracellular sodium, but can only record the overall total sodium ions concentration. Changes can be the result of altered volume fractions or altered intra and extra cellular concentrations. Moreover, the spatial resolution of sodium imaging at 3T is poor (with a nominal

resolution of 4x4x4mm^3), which implies that our measurements are currently affected by partial volume effects, requiring specific assessment of the point spread function for correction (Thulborn, 2018). Furthermore, the functional paradigm is non-standard and would benefit from faster image acquisition methods to increase the temporal resolution of the experiment, hence a limitation that needs overcoming. Nevertheless, the results presented here are all statistically significant and FWE corrected ($p<0.001$, 20 voxels).

Beyond what has been discussed so far, one could speculate on the tissue composition of an imaging voxel further and try to assess the potential contribution to ΔTSC coming from many compartments, defining e.g. fractions of the axonal volume, soma, myelin, extra cellular matrix, VRSV (or CSF) space and CBV. A comprehensive model should also consider exchange of sodium ions at synaptic level and for the functioning of other cells that contain sodium ions such as glial cells. Moreover, a model that would assess the fNaI source of signal changes would need to be adapted for different brain regions and would be expected also to differ depending on the functional task. Therefore, it is essential that future studies are planned in order to exclude or estimate the contribution of specific compartments to signal changes, either experimentally or through realistic computational modeling that take into consideration action potential associations to sodium ion flux, neurovascular coupling and compartmentalisation changes during activity for specific cortical regions (Alahmadi et al., 2017).

Confidence in the potential power of quantitative fNaI comes from the exceptional coherence of the ΔTSC values found in the cerebellar and primary motor cortex (0.54 vs 0.46 mmol/l), which is halved in the corpus callosum (0.27 mmol/l) where there are only white matter fibres, and is negative (-11 mmol/l) in the ipsilateral primary motor cortex where we would expect inhibitory mechanisms to (Hamzei et al., 2002) effectively reduce background firing activity.

This is a framework essential for advancing our understanding of the human brain function, where knowledge must bridge gaps between cellular and large-scale systems (D'Angelo and Wheeler-Kingshott, 2017). This study aimed to be a proof of principle, while dedicated major efforts should be employed to speed up acquisition and at the same time improve spatial resolution of sodium imaging, which is a major limitation of sodium imaging in general. Potentially, this emerging and exciting field of research could greatly benefit from higher field strength systems (e.g. 7T) (Ranjeva et al., 2018; Riemer et al., 2015).

In conclusion, sodium changes during activity are significantly large to be detected and more importantly quantified using fNaI *in vivo*. Improvements in data acquisition and computational modelling of neurovascular coupling in relation to sodium ions (23Na) flux during action potential generation and maintenance could open a new way forward to assess neuronal activation in humans *in vivo* non-invasively.

Acknowledgements

The NMR unit where this work was performed is supported by grants from the UK Multiple Sclerosis Society and is supported by the UCL/UCLH NIHR (National Institute for Health Research) BRC (Biomedical Research Centre). CGWK also receives funding from the Horizon2020 EU programme (H2020-EU.3.1 (634541)), ISRT, Wings for Life, CHNF. GC has an ECTRIMS fellowship. FPr was funded for the duration of this study by the Medical Research Council (MRC). FPr has a non-Clinical Postdoctoral Guarantors of Brain fellowship. FPa is supported by the Italian Ministry of Health (NET2013-02355313). EDA receives grants from the Human Brain Project, Centro Fermi and the Italian Ministry of Health.

References

Alahmadi, A. A. S., Samson, R. S., Pardini, M., D'Angelo, E., Friston, K. J., Toosy, A. T., et al. (2017). Investigating the relationship between multiple grip forces and BOLD signal in the Cerebellum and dentate nuclei of MS subjects. *Front. Cell. Neurosci.* doi:10.3389/conf.fncel.2017.37.00004.

Brockhaus, J., Ballanyi, K., Smith, J. C., and Richter, D. W. (1993). Microenvironment of respiratory neurons in the in vitro brainstem???spinal cord of neonatal rats. *J. Physiol.* 462, 421–445. doi:10.1113/jphysiol.1993.sp019562.

Buxton, R. B. (2012). Dynamic models of BOLD contrast. *Neuroimage*. doi:10.1016/j.neuroimage.2012.01.012.

Chadderton, P., Margie, T. W., and Häusser, M. (2004). Integration of quanta in cerebellar granule cells during sensory processing. *Nature*. doi:10.1038/nature02442.

Christensen, J. D., Barrere, B. J., Boada, F. E., Vevea, J. M., and Thulborn, K. R. (1996). Quantitative Tissue Sodium Concentration Mapping of Normal Rat Brain. *Magn. Reson. Med.* 36, 83–89.

D'Angelo, E., and Wheeler-Kingshott, C. A. M. (2017). Modelling the brain: Elementary components to explain ensemble functions. *La Riv. del Nuovo Cim.*, 297–333.

Dover, K., Marra, C., Solinas, S., Popovic, M., Subramaniyam, S., Zecevic, D., et al. (2016). FHF-independent conduction of action potentials along the leak-resistant cerebellar granule cell axon. *Nat. Commun.* 7, 12895. doi:10.1038/ncomms12895http://www.nature.com/articles/ncomms12895#supplementary-information.

Gilles, A., Nagel, A. M., and Madelin, G. (2017). Multipulse sodium magnetic resonance imaging for multicompartment quantification: Proof-of-concept. *Sci. Rep.* 7. doi:10.1038/s41598-017-17582-w.

Giza, J., Urbanski, M. J., Prestori, F., Bandyopadhyay, B., Yam, A., Friedrich, V., et al. (2010). Behavioral and Cerebellar Transmission Deficits in Mice Lacking the Autism-Linked Gene Islet Brain-2. *J. Neurosci.* 30, 14805–14816. doi:10.1523/jneurosci.1161-10.2010.

Gurney, P. T., Hargreaves, B. A., and Nishimura, D. G. (2006). Design and analysis of a practical 3D cones trajectory. *Magn. Reson. Med.* 55–3, 575–582. doi:10.1002/mrm.20796.

Hamzei, F., Dettmers, C., Rzanny, R., Liepert, J., Büchel, C., and Weiller, C. (2002). Reduction of excitability ("inhibition") in the ipsilateral primary motor

cortex is mirrored by fMRI signal decreases. *Neuroimage*. doi:10.1006/nimg.2002.1077.
Häusser, M., and Clark, B. A. (1997). Tonic synaptic inhibition modulates neuronal output pattern and spatiotemporal synaptic integration. *Neuron*. doi:10.1016/S0896-6273(00)80379-7.
Howarth, C., Gleeson, P., and Attwell, D. (2012). Updated energy budgets for neural computation in the neocortex and cerebellum. *J. Cereb. Blood Flow Metab.* doi:10.1038/jcbfm.2012.35.
Howarth, C., Peppiatt-Wildman, C. M., and Attwell, D. (2009). The energy use associated with neural computation in the cerebellum. *J. Cereb. Blood Flow Metab.* 30, 403–414. doi:10.1038/jcbfm.2009.231.
Hua, J., Qin, Q., Pekar, J. J., and van Zijl, P. C. M. (2011). Measurement of absolute arterial cerebral blood volume in human brain without using a contrast agent. *NMR Biomed.* doi:10.1002/nbm.1693.
Kim, T., Hendrich, K. S., Masamoto, K., and Kim, S. G. (2007). Arterial versus total blood volume changes during neural activity-induced cerebral blood flow change: Implication for BOLD fMRI. *J. Cereb. Blood Flow Metab.* doi:10.1038/sj.jcbfm.9600429.
Koch, R. A., and Barish, M. E. (1994). Perturbation of intracellular calcium and hydrogen ion regulation in cultured mouse hippocampal neurons by reduction of the sodium ion concentration gradient. *J Neurosci*.
Leblond, C. S., Nava, C., Polge, A., Gauthier, J., Huguet, G., Lumbroso, S., et al. (2014). Meta-analysis of SHANK Mutations in Autism Spectrum Disorders: A Gradient of Severity in Cognitive Impairments. *PLOS Genet.* 10, e1004580. doi:10.1371/journal.pgen.1004580.
Lee, S. P., Duong, T. Q., Yang, G., Iadecola, C., and Kim, S. G. (2001). Relative changes of cerebral arterial and venous blood volumes during increased cerebral blood flow: Implications for bold fMRI. *Magn. Reson. Med.* doi:10.1002/mrm.1107.
Mak, M. K. Y., Cheung, V., Ma, S., Lu, Z. L., Wang, D., Lou, W., et al. (2016). Increased cognitive control during execution of finger tap movement in people with Parkinson's disease. *J. Parkinsons. Dis.* doi:10.3233/JPD-160849.
Mapelli, L., Gagliano, G., Soda, T., Laforenza, U., Moccia, F., and D'Angelo, E. (2016). Granular layer neurons control cerebellar neurovascular coupling through an NMDA receptor/NO — dependent system. *J. Neurosci.* doi:10.1523/jneurosci.2025-16.2016.
Masoli, S., Solinas, S., and D'Angelo, E. (2015). Action potential processing in a detailed Purkinje cell model reveals a critical role for axonal compartmentalization. *Front. Cell. Neurosci.* 9, 47. doi:10.3389/fncel.2015.00047.
Morrison, M. A., Tam, F., Garavaglia, M. M., Hare, G. M. T., Cusimano, M. D., Schweizer, T. A., et al. (2016). Sources of Variation Influencing Concordance between Functional MRI and Direct Cortical Stimulation in Brain Tumor Surgery. *Front. Neurosci.* 10. doi:10.3389/fnins.2016.00461.
Ogawa, S., Lee, T.-M., Nayak, A. S., and Glynn, P. (1990a). Oxygenation-sensitive contrast in magnetic resonance image of rodent brain at high magnetic fields. *Magn. Reson. Med.* 14, 68–78. doi:10.1002/mrm.1910140108.
Ogawa, S., Lee, T. M., Kay, A. R., and Tank, D. W. (1990b). Brain magnetic resonance imaging with contrast dependent on blood oxygenation. *Proc.*

Natl. Acad. Sci. U. S. A. 87, 9868–9872. Available at: http://www.ncbi.nlm.nih.gov/pmc/articles/PMC55275/.

Ogawa, S., Tank, D. W., Menon, R., Ellermann, J. M., Kim, S. G., Merkle, H., et al. (1992). Intrinsic signal changes accompanying sensory stimulation: functional brain mapping with magnetic resonance imaging. *Proc. Natl. Acad. Sci.* 89, 5951–5955. Available at: http://www.pnas.org/content/89/13/5951.abstract.

Paling, D., Thade Petersen, E., Tozer, D. J., Altmann, D. R., Wheeler-Kingshott, C. A. M., Kapoor, R., et al. (2013). Cerebral Arterial Bolus Arrival Time is Prolonged in Multiple Sclerosis and Associated with Disability. *J. Cereb. Blood Flow Metab.* 34, 34–42. doi:10.1038/jcbfm.2013.161.

Piechnik, S. K., Evans, J., Bary, L. H., Wise, R. G., and Jezzard, P. (2009). Functional changes in CSF volume estimated using measurement of water T2 relaxation. *Magn. Reson. Med.* doi:10.1002/mrm.21897.

Pipe, J. G. (2000). Reconstructing MR images from undersampled data: data-weighting considerations. *Magn Reson Med* 43(6), 867–875.

Powell, K., Mathy, A., Duguid, I., and Häusser, M. (2015). Synaptic representation of locomotion in single cerebellar granule cells. *Elife*. doi:10.7554/eLife.07290.

Rancz, E. A., Ishikawa, T., Duguid, I., Chadderton, P., Mahon, S., and Häusser, M. (2007). High-fidelity transmission of sensory information by single cerebellar mossy fibre boutons. *Nature*. doi:10.1038/nature05995.

Ranjeva, J.-P., Bydder, M., Ridley, B., Soubrier, M., Bertinetti, M., Guye, M., et al. (2018). Functional sodium (23Na) MRI at 7T - Extracellular sodium decreases during cortical activation in the human brain. in *Proc. Intl. Soc. Mag. Reson. Med. 26*, 707.

Riemer, F., Solanky, B. S., Golay, X., D'Angelo, E., and Wheeler-Kingshott, C. A. M. (2015). Sodium fMRI detects grey and white matter activations: neuronal firing or blood volume change? in *Proc. Intl. Soc. Mag. Reson. Med. 23*, 3924.

Riemer, F., Solanky, B. S., Stehning, C., Clemence, M., Wheeler-Kingshott, C. A. M., and Golay, X. (2014). Sodium ((23)Na) ultra-short echo time imaging in the human brain using a 3D-Cones trajectory. *MAGMA* 27, 35–46. doi:10.1007/s10334-013-0395-2.

Sakatani, K., Murata, Y., Fujiwara, N., Hoshino, T., Nakamura, S., Kano, T., et al. (2007). Comparison of blood-oxygen-level–dependent functional magnetic resonance imaging and near-infrared spectroscopy recording during functional brain activation in patients with stroke and brain tumors. *J. Biomed. Opt.* 12, 62110–62118. doi:10.1117/1.2823036.

Sokoloff, L., Reivich, M., Kennedy, C., Rosiers, M. H. Des, Patlak, C. S., Pettigrew, K. D., et al. (1977). The [14 C]Deoxyglucose Method for the Measurement of Local Cerebral Glucose Utilization: Theory, Procedure, and Normal Values in the Conscious and Anesthetized Albino Rat. *J. Neurochem.* doi:10.1111/j.1471-4159.1977.tb10649.x.

Suchorska, B., Weller, M., Tabatabai, G., Senft, C., Hau, P., Sabel, M. C., et al. (2016). Complete resection of contrast-enhancing tumor volume is associated with improved survival in recurrent glioblastoma—results from the DIRECTOR trial. *Neuro. Oncol.* 18, 549–556. doi:10.1093/neuonc/nov326.

Thulborn, K. R. (2018). Quantitative sodium MR imaging: A review of its evolving role in medicine. *Neuroimage*. doi:10.1016/j.neuroimage.2016.11.056.

Witt, S. T., Laird, A. R., and Meyerand, M. E. (2008). Functional neuroimaging correlates of finger-tapping task variations: An ALE meta-analysis. *Neuroimage*. doi:10.1016/j.neuroimage.2008.04.025.

Yoon, H. J., Park, K. W., Jeong, Y. J., and Kang, D. Y. (2012). Correlation between neuropsychological tests and hypoperfusion in MCI patients: Anatomical labeling using xj view and talairach daemon software. *Ann. Nucl. Med.* 26, 656–664. doi:10.1007/s12149-012-0625-0.

Figure and table captions

Table 1: Clusters of activations and identification of areas involved according to the Tailarach atlas in XJVIEW. In red are right (ipsilateral) clusters and in blue are left (contralateral) clusters with respect to the hand used for the task.

Figure 1: a) Example of transverse slices from a single functional sodium imaging (fNaI) volume after smoothing. The circles either side of the brain are known concentration phantoms. b) Activation clusters from proof of concept fNaI experiment where the subject performed a 1Hz finger-tapping paradigm. Results are from group analysis of 8 volunteers (FWE corrected, $p<0.001$, 20 voxels), overlaid on 3D T_1-weighted structural images with anatomical annotations. Activations are seen in motor-function related areas. c) The cerebellum shows enhanced activations in Crus I/II and lobule VI related to finger tapping and motor planning. GM: gray matter and WM: white matter.

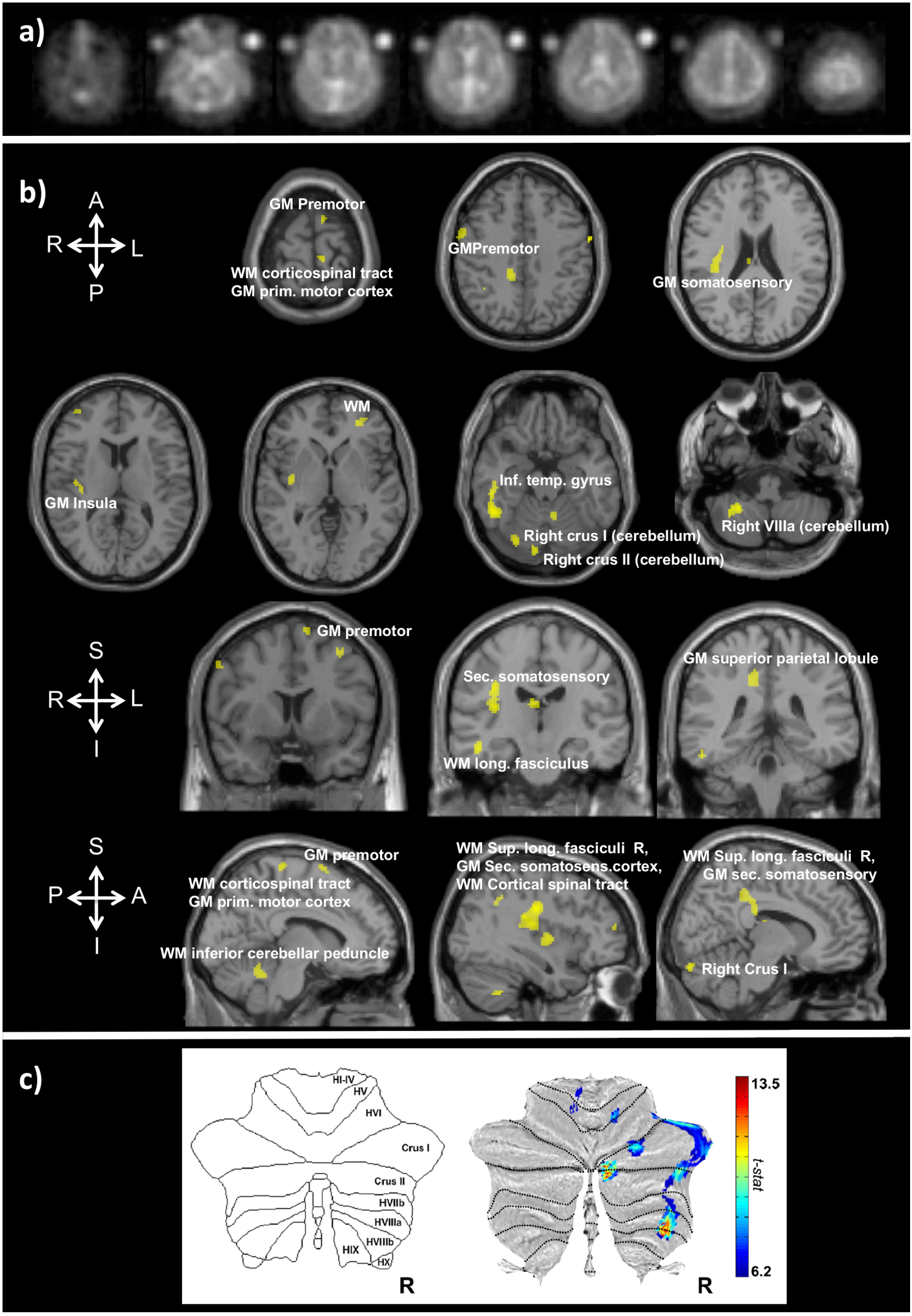
a)
b)
A
R
L
P
GM Premotor
WM corticospinal tract
GM prim. motor cortex
GMPremotor
GM somatosensory
GM Insula
WM
Inf. temp. gyrus
Right crus I (cerebellum)
Right crus II (cerebellum)
Right VIIIa (cerebellum)
S
R
L
I
GM premotor
Sec. somatosensory
WM long. fasciculus
GM superior parietal lobule
S
P
A
I
GM premotor
WM corticospinal tract
GM prim. motor cortex
WM inferior cerebellar peduncle
WM Sup. long. fasciculi R,
GM Sec. somatosens.cortex,
WM Cortical spinal tract
WM Sup. long. fasciculi R,
GM sec. somatosensory
Right Crus I
c)
HI-IV
HV
HVI
Crus I
Crus II
HVIIb
HVIIIa
HVIIIb
HIX
HX
R
13.5
t-stat
6.2
R

Table 1: Clusters of activations and identification of areas involved according to the Tailarach atlas in XJVIEW. In red are right (ipsilateral) clusters and in blue are left (contralateral) clusters with respect to the hand used for the task.

Cluster	N voxels	Peak MNI coordinates			Peak Description	Sub clusters
		X	Y	Z		
1	612	28	-50	-52	Right Cerebellum // Cerebellum Posterior Lobe // Cerebellar Tonsil // Cerebelum_8_R (aal)	Cerebellar Tonsil Cerebellum_8_R (aal) Inferior Temporal Gyrus brodmann area 37 Fusiform_R (aal) Cerebellum_Crus1_R (aal) Middle Temporal Gyrus Cerebellum Anterior Lobe
2	55	12	-86	-26	Right Cerebellum // Cerebellum Posterior Lobe // Declive //Cerebelum_Crus1_R (aal)	Declive Cerebellum_Crus1_R (aal) Cerebellum_Crus2_R (aal)
4	45	28	-74	-22	Right Cerebrum // Cerebellum Posterior Lobe // Declive	Declive Cerebelum_6_R (aal)
3	101	-8	-50	-28	Left Cerebellum // Cerebellum Anterior Lobe // Fastigium	Culmen Cerebelum_4_5_L (aal) Fastigium Dentate
5	55	18	-60	-10	Right Cerebrum // Occipital Lobe // Lingual Gyrus // White Matter //Lingual_R (aal)	Lingual_R (aal) brodmann area 19 White Matter Limbic Lobe Parahippocampa Gyrus Culmen Right Cerebellum Cerebellum Anterior Lobe
6	66	-36	48	-10	Left Cerebrum // Frontal Lobe // Middle Frontal Gyrus // White Matter // Frontal_Mid_Orb_L (aal)	Frontal_Mid_Orb_L (aal) Gray Matter brodmann area 11 Frontal_Sup_Orb_L (aal)
7	432	38	-18	26	Right Cerebrum // Sub-lobar // Extra-Nuclear // White Matter	White Matter Insula_R (aal) brodmann area 13 Extra-Nuclear Rolandic_Oper_R (aal) Heschl_R (aal) Frontal Lobe Putamen_R (aal)
8	20	44	52	4	Right Cerebrum // Frontal Lobe // Inferior Frontal Gyrus // White Matter // Frontal_Mid_R (aal)	Frontal_Mid_R (aal) Right Cerebrum White Matter
9	296	6	-18	14	Right Cerebrum // Sub-lobar // Thalamus // Gray Matter // Thalamus_R (aal)	White Matter Limbic Lobe Cingulate Gyrus Cingulum_Mid_R (aal) Sub-lobar Gray Matter Extra-Nuclear Thalamus_R (aal) Corpus Callosum Frontal Lobe
10	22	36	-48	36	Right Cerebrum // Parietal Lobe // White Matter	Supramarginal Gyrus
11	32	-60	0	36	Left Cerebrum // Frontal Lobe // Precentral Gyrus // brodmann area 6 // Precentral_L (aal)	brodmann area 6 Precentral_L (aal)
12	64	60	2	38	Right Cerebrum // Frontal Lobe // precentral Gyrus // Grey Matter // broadmann area 6 //	Precentral Gyrus brodmann area 6

					precentral_R (aal)	Inferior Frontal Gyrus Postcentral_R (aal)
13	26	-34	8	52	Left Cerebrum // Frontal Lobe // Middle Frontal Gyrus // Gray Matter // brodmann area 6 // Frontal_Mid_L (aal)	Frontal_Mid_L (aal) White Matter brodmann area 6
14	24	-46	-32	58	Left Cerebrum // Parietal Lobe // Postcentral Gyrus // Gray Matter // brodmann area 2 // Postcentral_L (aal)	brodmann area 2 Postcentral_L (aal)
15	28	-8	8	68	Left Cerebrum // Frontal Lobe // Superior Frontal Gyrus // White Matter // Supp_Motor_Area_L (aal)	Superior Frontal Gyrus Supp_Motor_Area_L (aal) White Matter
16	25	-8	-28	68	Left Cerebrum // Frontal Lobe // Medial Frontal Gyrus // White Matter // Paracentral_Lobule_L (aal)	Paracentral_Lobule_L (aal) White Matter Medial Frontal Gyrus